Stable intronic sequence RNAs have possible regulatory roles in *Drosophila melanogaster*

Jun Wei Pek,[1] Ismail Osman,[1]* Mandy Li-Ian Tay,[1]* and Ruther Teo Zheng[2]

[1]Temasek Life Sciences Laboratory, National University of Singapore, Singapore 117604
[2]Ngee Ann Polytechnic, Singapore 599489

Stable intronic sequence RNAs (sisRNAs) have been found in *Xenopus tropicalis*, human cell lines, and Epstein-Barr virus; however, the biological significance of sisRNAs remains poorly understood. We identify sisRNAs in *Drosophila melanogaster* by deep sequencing, reverse transcription polymerase chain reaction, and Northern blotting. We characterize a sisRNA (*sisR-1*) from the *regena* (*rga*) locus and show that it can be processed from the precursor messenger RNA (pre-mRNA). We also document a cis-natural antisense transcript (*ASTR*) from the *rga* locus, which is highly expressed in early embryos. During embryogenesis, *ASTR* promotes robust *rga* pre-mRNA expression. Interestingly, *sisR-1* represses *ASTR*, with consequential effects on *rga* pre-mRNA expression. Our results suggest a model in which *sisR-1* modulates its host gene expression by repressing *ASTR* during embryogenesis. We propose that *sisR-1* belongs to a class of sisRNAs with probable regulatory activities in *Drosophila*.

Introduction

Noncoding RNAs (ncRNAs) have emerged as potent agents that regulate diverse processes during normal development (Matera et al., 2007; Lee, 2012; Rinn and Chang, 2012; Kung et al., 2013; Cech and Steitz, 2014). Introns are noncoding sequences interspersed between the coding exons in most genes of higher eukaryotes. During transcription, intronic RNAs are spliced from the precursor mRNAs (pre-mRNAs) by the splicing machinery (Wahl et al., 2009; Hoskins and Moore, 2012). Whereas mature mRNAs are exported to the cytoplasm, intronic RNAs remain in the nucleus, where they are rapidly degraded (Sharp et al., 1987; Clement et al., 1999). However, intronic RNAs can also be processed into functional ncRNAs, such as the small nucleolar RNAs (snoRNAs), small Cajal body-specific RNAs, and certain miRNAs (Liu and Maxwell, 1990; Leverette et al., 1992; Tycowski et al., 1993; Berezikov et al., 2007; Kim and Kim, 2007; Matera et al., 2007; Okamura et al., 2007; Ruby et al., 2007; Brown et al., 2008). They function in guiding modification of ribosomal RNA (rRNA) and small nuclear RNA or in regulating gene expression (Bushati and Cohen, 2007; Matera et al., 2007). Furthermore, intronic RNAs in plants and mammalian cell cultures may also function as long ncRNAs to modulate transcription and splicing (Heo and Sung, 2011; Guil et al., 2012; Yin et al., 2012; Zhang et al., 2013).

Recently, a class of ncRNAs called stable intronic sequence RNAs (sisRNAs) was discovered in the oocyte nucleus of the frog *Xenopus tropicalis* (Gardner et al., 2012). Soon after, sisRNAs were also found in human cell lines and the Epstein-Barr virus (Yin et al., 2012; Moss and Steitz, 2013; Zhang et al., 2013). Although the phenomenon is evolutionary conserved, the functions of sisRNAs during development remain poorly understood. Here we identify sisRNAs and present evidence for processing and a function of a sisRNA (*sisR-1*) in *Drosophila melanogaster*. We show that *sisR-1* can be processed from the *regena* (*rga*) pre-mRNA, and nuclear *sisR-1* is further processed at the 3′ end to form cytoplasmic *sisR-1*. During embryogenesis, *sisR-1* represses the expression of a cis-natural antisense transcript (cis-NAT) called antisense transcript of *rga* (*ASTR*), and *ASTR* promotes the expression of the *rga* pre-mRNA. Therefore, our data suggest a regulatory loop whereby *sisR-1* modulates *rga* pre-mRNA expression by repressing *ASTR* during embryogenesis in *Drosophila*.

Results and discussion

Identification of sisRNAs

The *Drosophila* early embryo constitutes an excellent system for identification of sisRNAs because it contains a store of mature and stable RNA molecules. During oogenesis, each egg chamber consists of a growing oocyte and 15 nurse cells surrounded by a sheet of somatic follicle cells (Fig. 1 A). Whereas the germinal vesicle is transcriptionally quiescent, the oocyte receives and stores RNAs from the transcriptionally active polyploid

*I. Osman and M.L.-I. Tay contributed equally to this paper.

Correspondence to Jun Wei Pek: junwei@tll.org.sg

Abbreviations used in this paper: cis-NAT, cis-natural antisense transcript; ncRNA, noncoding RNA; qPCR, quantitative PCR; pre-mRNA, precursor mRNA; rRNA, ribosomal RNA; sisRNA, stable intronic sequence RNA; snoRNA, small nucleolar RNA; RACE, rapid amplification of cDNA ends.

The Rockefeller University Press $30.00
J. Cell Biol. Vol. 211 No. 2 243–251
www.jcb.org/cgi/doi/10.1083/jcb.201507065

nurse cells (Spradling, 1993). Beginning from stage 10 of oogenesis, massive dumping of RNAs from the nurse cells to the oocyte occurs. A stage 10 egg chamber takes ∼10 h to develop into a stage 14 oocyte, during which time most of the stored RNAs persist (Lasko, 2012). Because zygotic transcription does not begin until 2 h after egg laying, most mature RNAs present in the 0–2 h embryo must have been stable for at least 10–12 h.

To identify candidate sisRNAs, we examined RNAs from 0–2-h embryos by deep sequencing. Total RNA was extracted, depleted of rRNA, and subjected to deep sequencing. Reads that were mapped to the introns of each gene were retrieved bioinformatically and analyzed manually. From a list of genes with intronic reads, candidate sisRNAs were identified using the following criteria. First, the intronic reads should display a distinct peak on the genome browser. Second, with reference to the FlyBase annotation (Dmel Release 6), the intronic reads should not derive from retained introns of alternatively spliced isoforms. Finally, the reads should not map to intronic or overlapping protein-coding genes and ncRNAs (including mirtrons, snoRNAs, and long ncRNAs). Using these criteria, we identified 34 candidate sisRNAs in the 0–2-h embryo (Table S1).

Because we used 0–2-h embryos for deep sequencing, which might be contaminated with some late-stage embryos and therefore pre-mRNAs from zygotic transcription, we verified our candidates using unfertilized eggs, which contain a pool of stable and mature RNAs. By RT-PCR, we verified the presence of 31 out of 34 candidates (>90%; Fig. 1 B and Fig. S1 A). We also examined the possibility that some of these sisRNAs may be RNase R resistant, implying that they may be circular. We tested six sisRNAs, and three appeared to have some populations of them being RNase R resistant (Fig. 1 C), suggesting the presence of both linear and circular sisRNAs. We further examined the expression patterns of three sisRNAs by Northern blotting. Expression of the *mushroom bodies tiny* (*mbt*) sisRNA was detected primarily in the ovaries and early embryos and dropped gradually as the embryos developed (Fig. 1 D, Fig. S1 B), suggesting that its expression is more restricted to the female germ line. A sisRNA from the *cysteine string protein* (*csp*) gene is highly abundant in third instar larvae, pupae, and adult somatic tissues (Fig. 1 D). However, we could not detect its expression in the early embryos, suggesting that its abundance was below the detection level of Northern blotting. Finally, we observed expression of *Ribosomal protein S27* (*RpS27*) sisRNA at a low level during development and in adult male somatic tissues (Fig. 1 D). Our data demonstrate that the expression of sisRNAs is not oocyte specific and that individual sisRNAs display extensive variation in their expression patterns during development and in adult tissues.

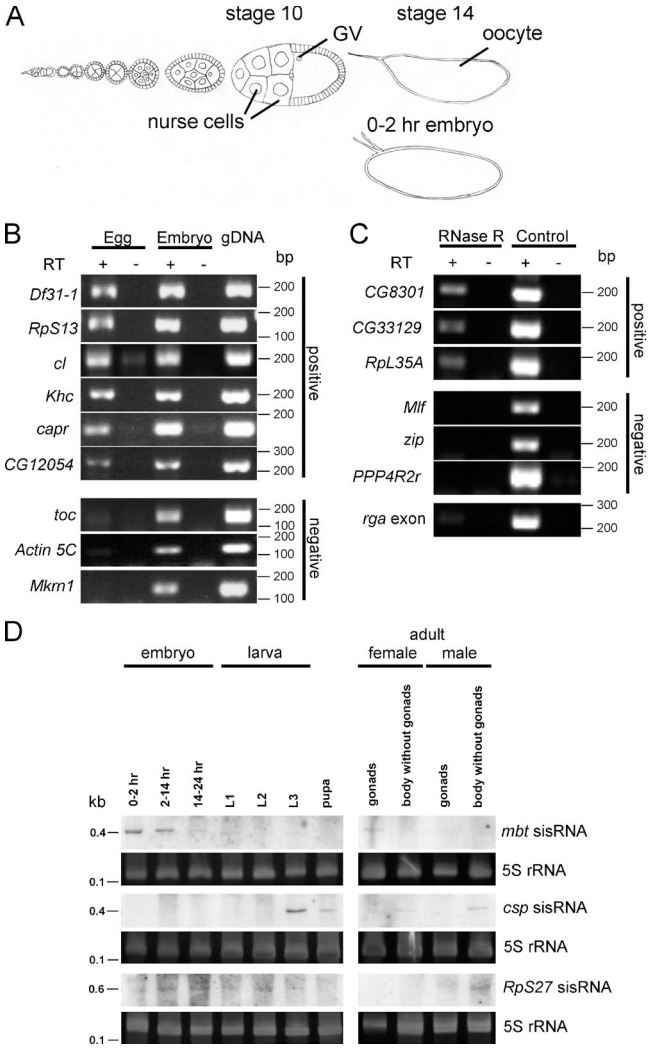

Figure 1. **Identification of sisRNAs.** (A) Diagram of an ovariole showing stages in the development of the oocyte and its accompanying nurse cells. Also shown is a 0–2-h embryo. GV, germinal vesicle. (B) RT-PCR showing expression of some sisRNAs in unfertilized eggs. (C) RT-PCR showing expression of some RNase R-resistant sisRNAs in unfertilized eggs. *rga* exon was used as a positive control for RNase R activity. (D) Northern blots showing expression of *mbt, csp,* and *RpS27* sisRNAs during development and in adult somatic tissues and gonads. The gels were stained with SYBR Gold to visualize 5S rRNA as a loading control. L1, first instar larvae; L2, second instar larvae; L3, third instar larvae.

sisRNA (*sisR-1*) from the *rga* locus

We focused on a candidate sisRNA from the fourth intron of the *rga* gene locus (Fig. 2 A). The *rga* gene encodes for the NOT2 protein, a component of the CCR4-NOT deadenylase complex (Frolov et al., 1998). We performed strand-specific RT-PCR using primers within the intronic and exonic peaks (Fig. 2 A) and found that the sisRNA is transcribed from the coding strand (Fig. 2 B). To determine whether the intronic peak represents a sisRNA of discrete size, we performed Northern blotting using two probes that target different regions of the intron. Probe A spans the region within the intronic peak, whereas probe B derives from the region that lacks reads and served as a negative control (Fig. 2 A). We detected a band of ∼300 nucleotides with probe A using RNA from 0–2-h embryos, whereas probe B gave no signal (Fig. 2 C). These results demonstrated that the sequences seen on the browser derive from a discrete sisRNA. Furthermore, expression was also detected in ovaries and unfertilized eggs (Fig. 2 C and Fig. S1 A), suggesting that the sisRNA is maternally deposited. We named this sisRNA *sisR-1* for the first sisRNA to be characterized in *D. melanogaster*. Interestingly, *sisR-1*, similar to its cognate *rga* mRNA, is ubiquitously expressed in embryos, larvae, pupae, and adult gonadal and somatic tissues and appears to be developmentally regulated (Fig. 2 D and Fig. S2, A and B).

To determine the stability of *sisR-1*, we examined RNA from ovaries that had been treated with actinomycin D to inhibit transcription. Incubation for 30 min was sufficient to inhibit transcription as assayed by 5-ethynyluridine staining (Fig. S2 C; Jao and Salic, 2008). We observed little or no change in *sisR-1*

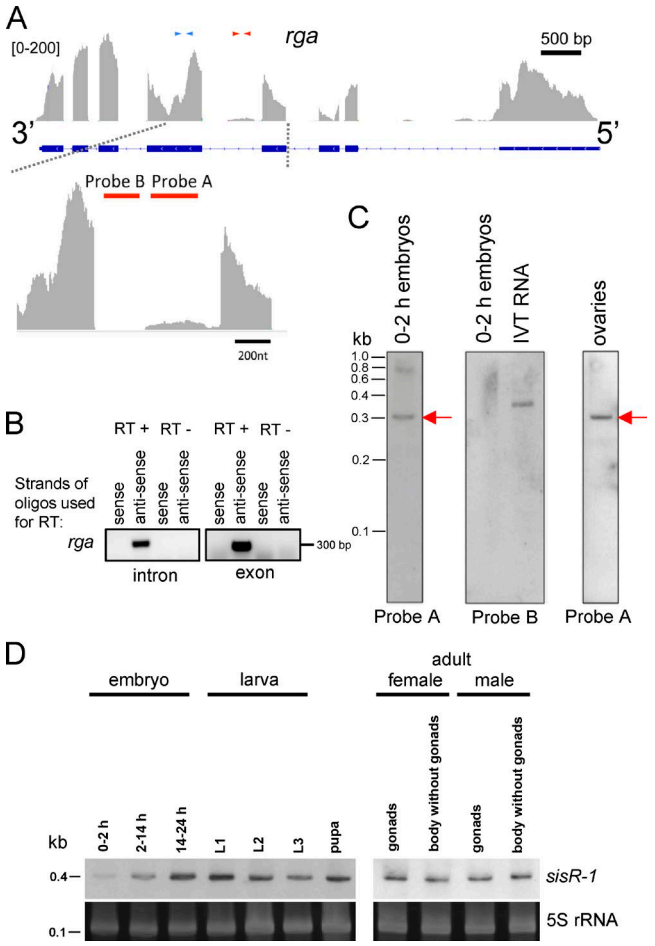

Figure 2. **sisRNA (*sisR-1*) from the *regena* locus.** (A) Genome browser view of exonic and intronic sequences in the *rga* locus. Blue and red arrows indicate exonic and intronic primers used for RT-PCR. The bottom panel shows an enlarged view of the intronic peak. Red bars indicate the regions to which probes A and B hybridize. (B) Strand-specific RT-PCR using primers in the intron and exon of *rga*. (C) Northern blots using probes A and B to detect expression of *sisR-1* in 0–2 h embryos and ovaries are shown. A band of ~300 nt was detected with probe A (red arrows). Probe B gave no detectable signal in RNA from 0–2-h embryos but did hybridize with 10 pg of in vitro transcribed (IVT) RNA. (D) Northern blots showing expression of *sisR-1* during development and in adult somatic tissues and gonads. The gels were stained with SYBR Gold to visualize 5S rRNA as a loading control. L1, first instar larvae; L2, second instar larvae; L3, third instar larvae.

levels after 120 min of actinomycin D treatment compared with a partial loss of an unstable species of RNA, *gypsy* retrotransposon mRNA (Fig. S2 D), which is negatively regulated by the piwi-interacting RNA pathway (Sarot et al., 2004). This result indicated that *sisR-1* was relatively more stable than *gypsy* mRNA. In *X. tropicalis*, the abundance of sisRNAs was estimated to be ~1% of the cognate mRNAs (Gardner et al., 2012). We performed the same analysis based on the peak heights of *sisR-1* and *rga* mRNA on the browser (Fig. 2 A) and found that the amount of *sisR-1* is ~5% that of *rga* mRNA. We also estimated the relative abundance of *sisR-1*, lariats, and pre-mRNAs in 2–14-h embryos. By Northern blotting we could only detect the presence of *sisR-1* but not the lariats and pre-mRNAs (Fig. S2 E), consistent with the idea that *sisR-1* is a more stable molecule. We estimated that there are ~2 × 10^7 molecules of *sisR-1* in 10 µg of total RNA.

sisR-1 can be processed from the *rga* pre-mRNA

Intronic ncRNAs can be cotranscribed and processed with the cognate pre-mRNA or independently transcribed from its own promoter (Okamura et al., 2007; Ruby et al., 2007; Brown et al., 2008; Heo and Sung, 2011; Yin et al., 2012). Recent studies have provided evidence that sisRNAs are not independently transcribed molecules in *Xenopus* and mammalian cell lines (Gardner et al., 2012; Yin et al., 2012; Zhang et al., 2013). We therefore asked if *sisR-1* can be processed from its cognate pre-mRNA. We used a P-element insertion line EY10731 that allows Gal4-inducible expression of the *rga* pre-mRNA (Fig. 3 A). Overexpression of *rga* pre-mRNA in the ovaries by *MTD-Gal4*, led to a concomitant increase in expression of *sisR-1* (Fig. 3 B), consistent with the idea that the *rga* pre-mRNA is processed into *sisR-1*. To ask whether the full-length intronic sequence itself is sufficient to produce *sisR-1*, we cloned both full length isoforms of the *rga* fourth intron. Long and short *rga* introns differ by their 5′ splice sites, with intact splice sites in between coding sequences of *dsRed* and *myc* (Fig. 3 C; Okamura et al., 2007) and generated transgenic flies. Overexpression of both intron isoforms in the ovaries by *MTD-Gal4* resulted in increased expressions of *sisR-1* (Fig. 3 D), indicating that the intronic sequence itself is sufficient to generate *sisR-1*. To test whether the *rga* intron contains an independent promoter, and the transgene insertion has any effect on endogenous *sisR-1* expression, we examined the levels of *sisR-1* in control (*y w*) versus *UAS-rga intron-L-myc* (without Gal4 induction) females. We did not detect any differences in *sisR-1* levels (Fig. S2 F), therefore excluding the presence of an intronic promoter and indirect effect of transgene insertion.

Because snoRNAs and mirtrons are processed from spliced intronic transcripts and require lariat debranching (ldbr) enzyme activity for their biogenesis (Brown et al., 2008), we asked whether *ldbr* is required for the production of *sisR-1*. Knockdown of *ldbr* in third instar larvae using a previously published *ldbr* RNAi transgenic fly (Conklin et al., 2005; Okamura et al., 2007) by *act-Gal4* resulted in a decrease in expression of *sisR-1* (Fig. 3 E). Importantly, we also observed a concomitant accumulation of higher molecular weight precursors, which were presumably the intron lariats (Fig. 3 E, arrowhead). Collectively, our data are consistent with a model in which *sisR-1* is processed from a predominant pathway that requires canonical splicing and debranching of intron lariats (Fig. 3 F).

3′ end processing of *sisR-1*

To determine whether *sisR-1* localizes to the nucleus or cytoplasm, we collected 14–24-h embryos where *sisR-1* expression is the highest during embryogenesis and performed nuclear-cytoplasmic fractionation. Relatively clean nuclear and cytoplasmic fractions were obtained as revealed by nuclear-specific expression of U85 and cytoplasmic-enrichment of 18S and 28S rRNA (Fig. 3 G). We performed Northern blotting and detected *sisR-1* in both the nuclear and cytoplasmic fractions (Fig. 3 G). Curiously, cytoplasmic *sisR-1* migrated faster than nuclear *sisR-1*, suggesting that they had different sizes (Fig. 3 G). It further implies processing of nuclear *sisR-1* to produce cytoplasmic *sisR-1*.

Both nuclear and cytoplasmic *sisR-1* were susceptible to RNase R-mediated degradation, indicating that they are not circular molecules or lariats (Fig. S2 G). We therefore mapped the ends of nuclear *sisR-1* by 5′ and 3′ rapid amplification of cDNA

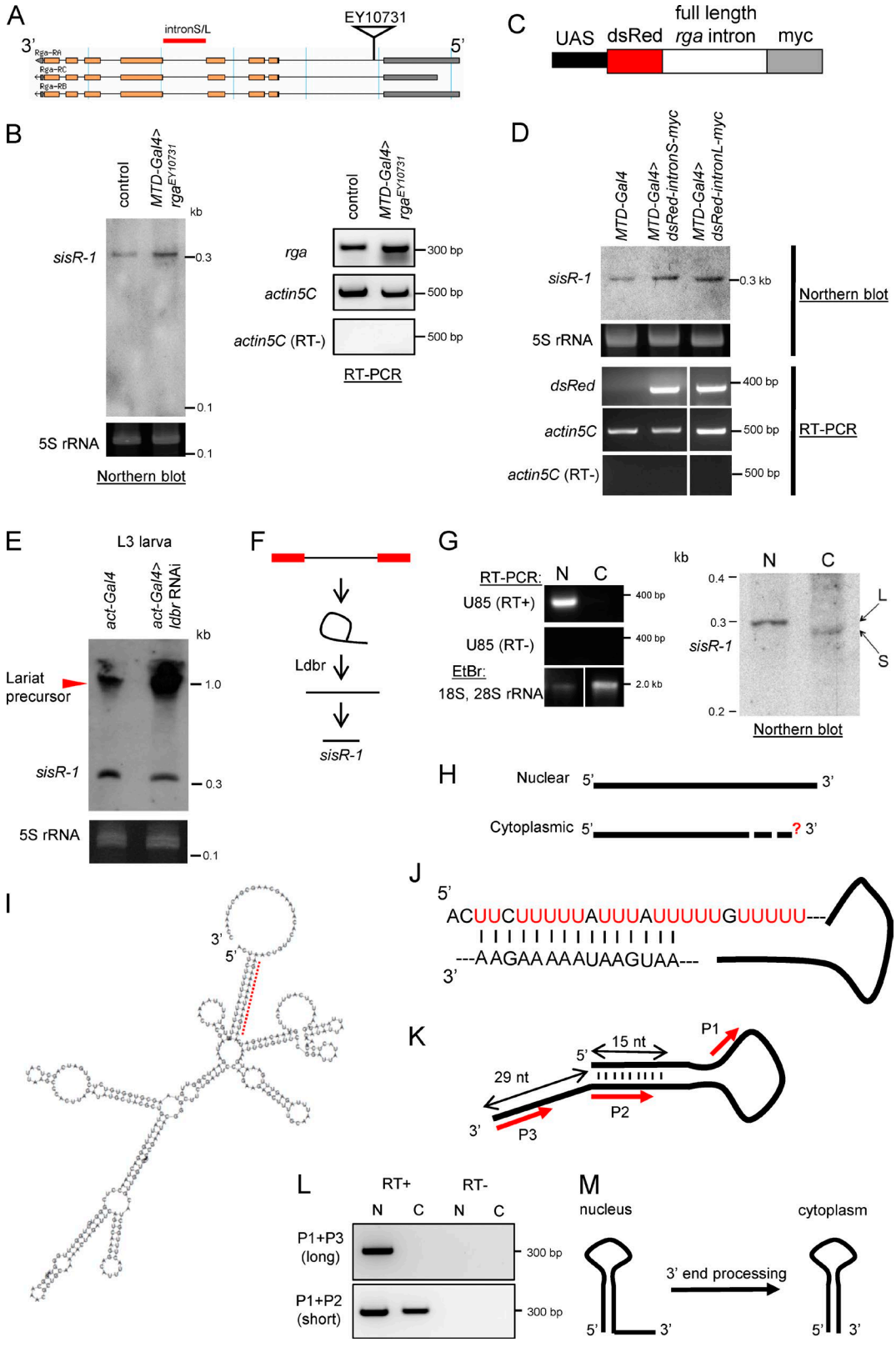

Figure 3. **Processing of *sisR-1*.** (A) Diagram showing the insertion of an EP element EY10731 used to overexpress the *rga* pre-mRNA. L, long; S, short. (B) A Northern blot showing expression of *sisR-1* in the ovaries of controls versus *rga* overexpression flies. RT-PCR showing expression of *rga* mRNA and *actin5C* in the ovaries of controls versus *rga* overexpression flies. (C) Diagram showing the construct used to overexpress *rga* intronic sequences. (D) Northern blot showing expression of *sisR-1* in ovaries of controls versus *rga* intronic sequence overexpression flies. RT-PCR verifies expression of *dsRed* mRNA in the ovaries of *dsRed-intron-myc* overexpression flies but not in controls. (E) Northern blots showing expression of *sisR-1* in the controls versus *ldbr* RNAi third instar larvae. (F) Model for processing of *sisR-1* from the *rga* pre-mRNA. (G) Northern blot showing detection of *sisR-1* in both the nuclear (N) and cytoplasmic (C) fractions of 14–24-h embryos. RT-PCR showing the expression of U85 only in the nuclear fraction. EtBr staining showing the enrichment of

ends (RACE) to determine its full-length sequence (Fig. S2 H). Using the same method, we found that cytoplasmic and nuclear *sisR-1* have the same 5′ end (Fig. 3 H). However, despite various attempts, we were unable to map the 3′ end of cytoplasmic *sisR-1*, probably because of the presence of an unknown RNA modification at the 3′ end, which made it technically difficult (Raabe et al., 2014). We next used the Vienna RNA fold web server to predict the secondary structure of nuclear *sisR-1*. The 5′ end of nuclear *sisR-1* contains a U-rich tract that was predicted to form 15 nucleotide base-pairing with a region near its 3′ end, leaving behind an exposed 3′ tail of 29 nucleotides (Fig. 3, I and J). Collectively, our findings suggest a possibility that cytoplasmic *sisR-1* is formed by 3′ end processing of nuclear *sisR-1*. To test this idea, we designed primers that anneal to different regions of the 3′ end of nuclear *sisR-1* (P2 anneals to both long and short *sisR-1* and P3 anneals specifically to long *sisR-1*; Fig. 3 K). By performing RT-PCR using the different primer pairs, we detected the presence of short, but not long, *sisR-1* in the cytoplasm (Fig. 3 L), verifying that cytoplasmic *sisR-1* is formed by 3′ end processing (Fig. 3 M).

ASTR promotes the expression of *rga* pre-mRNA

To search for potential molecular functions of *sisR-1*, we examined the genome organization of the *rga* locus. There is an annotated long ncRNA CR43628 transcribed in the antisense orientation with respect to *rga* (Fig. 4 A). We named this cis-NAT *ASTR*. The 3′ end of *ASTR* is predicted to form a 76-nucleotide base pairing with the 3′ end of nuclear *sisR-1* (Fig. 4 A), suggesting that *sisR-1* may bind to and regulate *ASTR*. Furthermore, the predicted secondary structure of *sisR-1* suggests that the 3′ end of nuclear *sisR-1* has an exposed 29 nt tail, further raising the possibility that it may bind to *ASTR* in the nucleus. By performing Northern blotting using a probe that is specific to *ASTR* (Fig. 4 A), we found that *ASTR* was highly expressed in 2–14-h embryos (Fig. 4 B). *ASTR* was also found to be predominantly in the nucleus as assayed by strand-specific RT-PCR (Fig. 4 C).

cis-NATs have been shown to regulate the expression of pre-mRNAs of their cognate genes by various mechanisms in different contexts (Wight and Werner, 2013; Herzog et al., 2014; Xue et al., 2014). *ASTR* and *rga* show similar expression patterns during embryogenesis, where both are highly expressed in the 2–14-h embryos and expression levels drop in the 14–24-h embryos and later developmental stages (Figs. 4 B and 5 D; and Fig. S2, A and B). This suggests a possibility that *ASTR* promotes *rga* pre-mRNA expression. We therefore tested whether *ASTR* has a role in regulating the *rga* pre-mRNA expression. We designed a shRNA that specifically targets *ASTR* under the UASp promoter and drove the expression in the embryos using *da-Gal4*. Expression of *ASTR* shRNA resulted in a robust knockdown of *ASTR* in 2–14-h embryos as assayed by Northern blotting (Fig. 4 D). By performing quantitative PCR (qPCR), we observed a significant decrease in the expression of *rga* pre-mRNA in *ASTR* RNAi 2–14-h embryos compared with controls (Fig. 4 E). This result could not have been the result of an indirect knockdown of *rga* pre-mRNA by the passenger strand because we and others had shown that shRNAs do not target pre-mRNAs (Fig. S3, A and B; discussed in the following section; Yin et al., 2012; Zhang et al., 2013). Therefore, our data suggest that *ASTR* plays a role in promoting robust *rga* pre-mRNA expression during embryogenesis.

sisR-1 represses the expression of *ASTR*

The expression pattern of *ASTR* during a specific window of 2–14-h embryogenesis suggests a mechanism that facilitates robust downregulation of *ASTR* during late embryogenesis (14–24 h). Interestingly, expression of *sisR-1* increased gradually during embryogenesis and peaked only at 14–24 h (Fig. 2 D). These reciprocal expression patterns between *sisR-1* and *ASTR* during embryogenesis suggest that *sisR-1* may facilitate the robust downregulation of *ASTR* during late embryogenesis.

We overexpressed *sisR-1* in 2–14-h embryos by driving *UAS-dsRed-rga intronL-myc* with *da-Gal4*, and we observed a robust downregulation of *ASTR* (Fig. 5 A). This result indicated that *sisR-1* acts in trans to repress *ASTR*. Further supporting a role for *ASTR* in promoting *rga* pre-mRNA expression, we also observed a concomitant drop in *rga* pre-mRNA expression in *sisR-1*–overexpressing 2–14-h embryos (Fig. 5 B).

We generated transgenic flies expressing two independent shRNAs that target specifically to two regions of *sisR-1* under the UASp promoter. Expression of *sisR-1* shRNAs driven by *da-Gal4* in ovaries resulted in four- to fivefold decrease in *sisR-1*, but not the *rga* pre-mRNA levels (Fig. S3, A and B), consistent with published studies that shRNAs specifically target sisRNAs but not pre-mRNAs (Yin et al., 2012; Zhang et al., 2013). This result indicates that the knockdown was specific to *sisR-1* but not the *rga* pre-mRNA. Next, we tested the idea that *sisR-1* may facilitate robust downregulation of *ASTR* during late embryogenesis. In support of this idea, we observed a delay in the downregulation of *ASTR* during 14–24-h embryogenesis in *sisR-1* RNAi embryos, but not in controls (Fig. 5 C). The hatching rates of *sisR-1* RNAi embryos were similar to that of the controls (Fig. S3 C), indicating that the delay in downregulation of *ASTR* was not the result of a delay in developmental progression.

In control embryos, the expression of *rga* pre-mRNA decreases from 2–14 h to 14–24 h (Fig. 5 D), which correlates with a decrease in the expression of *ASTR* (Fig. 4 B). Because we observed a less robust downregulation of *ASTR* in *sisR-1* RNAi embryos, and *ASTR* promotes *rga* pre-mRNA expression, we asked if the downregulation of *rga* pre-mRNA was also perturbed. As assayed by qPCR, the downregulation of *rga* pre-mRNA from 2–14-h to 14–24-h embryos was significantly perturbed in *sisR-1* RNAi embryos (Fig. 5 D). Importantly, the failure to downregulate *rga* pre-mRNA in *sisR-1* RNAi embryos was rescued by simultaneously knocking down *ASTR*, indicating that the effect was mediated by *ASTR* (Fig. 5 D). Therefore, our data suggest that *sisR-1* represses *ASTR* to promote robust downregulation of *rga* pre-mRNA from 2–14-h to 14–24-h embryogenesis (Fig. 5 E).

18S, 28S rRNA in the cytoplasmic fraction. RNAs were run on the same gel, and the intervening lanes were removed (white vertical lines). (H) Diagram showing the 5′ and 3′ ends of the nuclear and cytoplasmic *sisR-1* determined by RACE. Question mark depicts unknown 3′ end of cytoplasmic *sisR-1*. (I) Predicted structure of nuclear *sisR-1* by Vienna RNA fold software. Red dotted region is shown in J. (J) Magnified view of the dotted region in I shows the base pairing. (K) Diagram with red arrows to indicate regions where the primers anneal to. (L) RT-PCR showing the detection of the short, but not long, isoform of *sisR-1* in the cytoplasmic fraction. (M) Model showing the processing of nuclear *sisR-1* to cytoplasmic *sisR-1* by 3′ end processing.

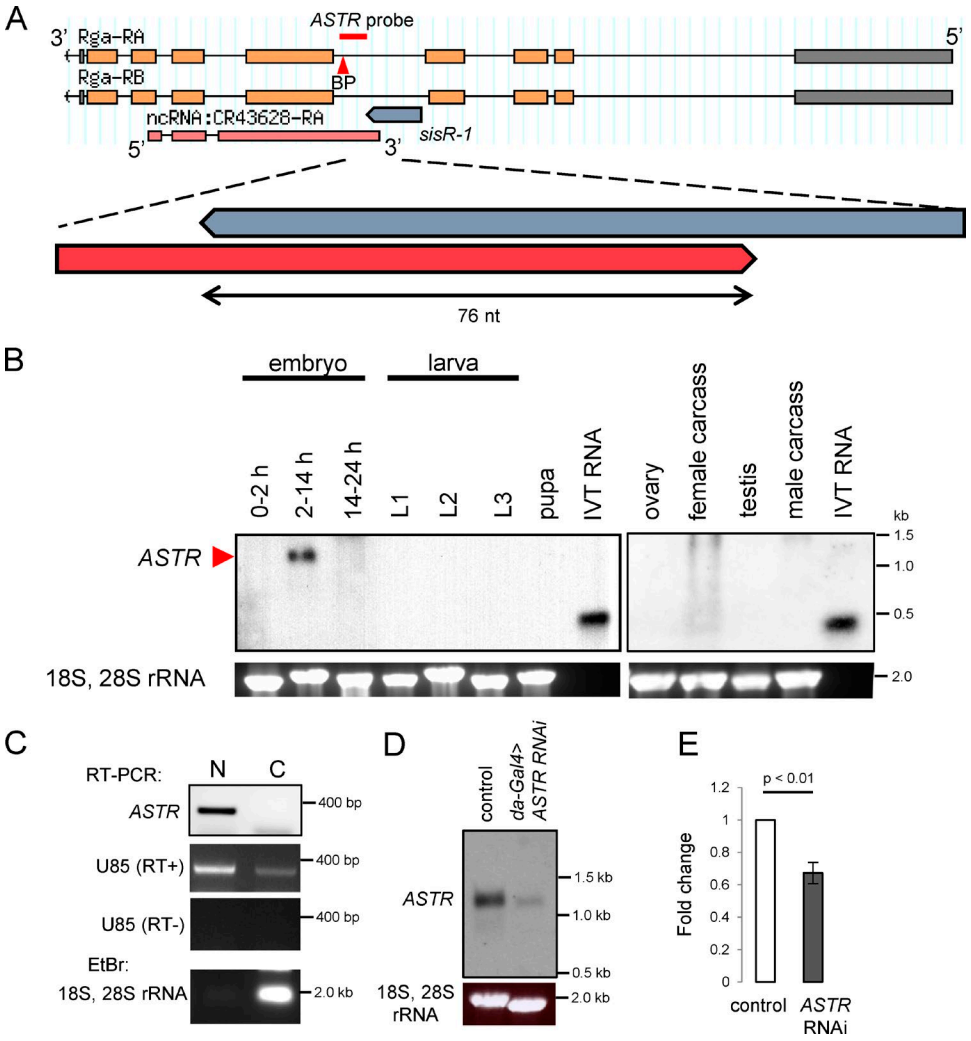

Figure 4. ***ASTR*promotes robust expression of *rga* pre-mRNA.** (A) Genomic locus showing regions of *rga*, *sisR-1*, and *ASTR*. Red bar indicates the region where the *ASTR* probe binds. Red arrowhead points to a putative branch point (BP) CTAAT. (B) Northern blots showing expression of *ASTR* in 2–14-h embryos. In vitro transcribed (IVT) RNA was used as positive controls. The gels were stained with EtBr to visualize 18S, 28S rRNA as a loading control. (C) Strand-specific RT-PCR detecting the presence of *ASTR* in the nuclear but not the cytoplasmic fraction of 2–14-h embryos. RT-PCR showing the high expression of U85 in the nuclear fraction. EtBr staining showing the enrichment of 18S, 28S rRNA in the cytoplasmic fraction. (D) Northern blot showing the expression of *ASTR* in controls versus *da-Gal4>ASTR* RNAi 2–14-h embryos. The gel was stained with EtBr to visualize 18S, 28S rRNA as a loading control. (E) qPCR data showing relative expression of *rga* pre-mRNA normalized to *actin5C* in the controls versus *da-Gal4>ASTR* RNAi 2–14-h embryos. Error bars represent SD. $n = 3$. P-value represents *t* test.

In this study, we report a sisRNA (*sisR-1*) produced from the *rga* locus, likely processed from the *rga* pre-mRNA. *sisR-1* functions to repress the expression of *ASTR*, which is a positive regulator of the *rga* pre-mRNA. Collectively, our findings suggest a model whereby *sisR-1* modulates its host gene expression by repressing *ASTR* during embryogenesis in *Drosophila* (Fig. 5 E). Our results provide an explanation for the wild-type expression patterns of *sisR-1*, *ASTR*, and *rga* pre-mRNA from 2–14-h to 14–24-h embryos. During 2–14-h embryogenesis, a high level of *ASTR* promotes robust expression of *rga* pre-mRNA. A high level of *rga* pre-mRNA in turn contributes to production of more *sisR-1*. Over time, *sisR-1* accumulates to a level that is sufficient to repress *ASTR* during 14–24-h embryogenesis. Downregulation of *ASTR* then results in a lower expression of *rga* pre-mRNA. Therefore, *sisR-1* appears to modulate a negative feedback loop in promoting robust downregulation of its host gene during development. ncRNAs, such as miRNAs and long ncRNAs, have been shown to modulate gene expression via feedback loops (Herranz and Cohen, 2010; Peláez and Carthew, 2012; Xue et al., 2014). Feedback loops play important roles in biological systems to maintain a robustness network of gene expression. We propose that *sisR-1* is present in the nucleus to repress any uncontrolled accumulation of *ASTR*, which may have deleterious effects on *rga* expression.

Among the remaining sisRNA loci that we identified, only the *Decondensation factor 31* (*Df31*) locus have an annotated cis-NAT. It is possible that *Df31* sisRNAs regulate the cis-NAT in the same locus. Because *sisR-1* can act in trans, it is possible that other sisRNAs may have targets in trans that remain to be discovered. In general, sisRNAs may be present as a quality control and surveillance mechanism to target any antisense transcripts, which may affect gene expression.

In conclusion, we have shown that sisRNAs are present in *D. melanogaster* and characterized a novel sisRNA (*sisR-1*) that functions to modulate its host gene expression during embryogenesis by repressing a cis-NAT.

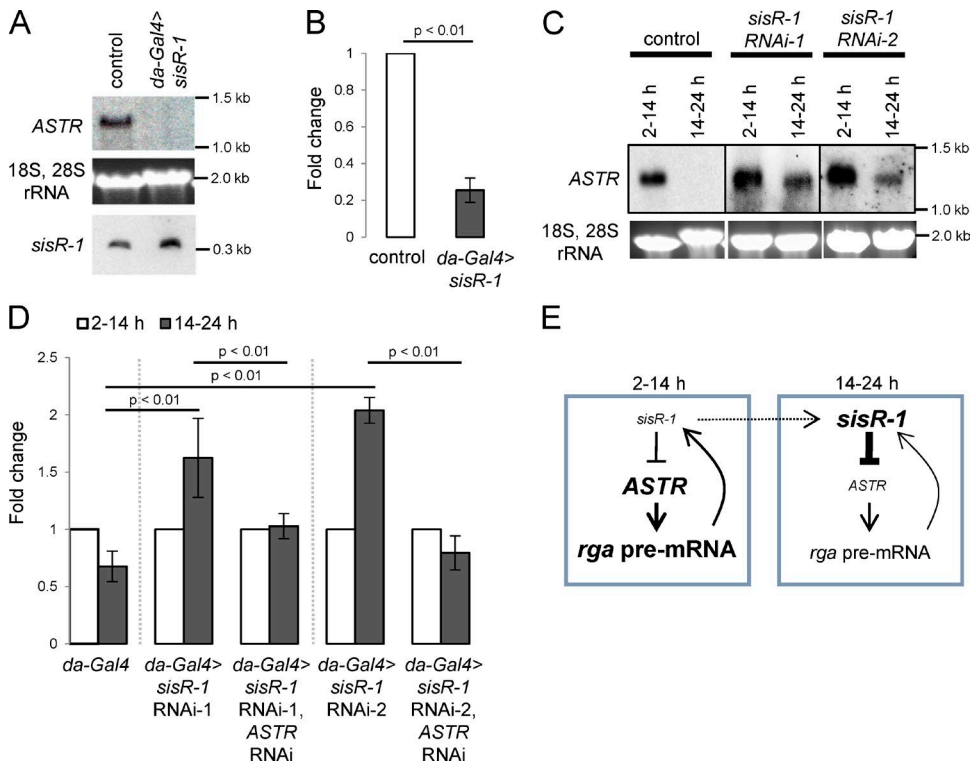

Figure 5. ***sisR-1*promotes robust repression of *ASTR*.** (A) Northern blot showing the expression of *ASTR* in controls versus *da-Gal4>sisR-1* 2–14-h embryos. (B) qPCR data showing relative expression of *rga* pre-mRNA normalized to *actin5C* in the controls versus *da-Gal4>sisR-1* 2–14-h embryos. Error bars represent SD. *n* = 3. P-value represents *t* test. (C) Northern blots showing expression of *ASTR* in controls versus embryos expressing *sisR-1* shRNA. The gels were stained with EtBr to visualize 18S, 28S rRNA as a loading control. (D) qPCR data showing fold change of *rga* pre-mRNA expression (normalized to *actin5C*) from 2–14-h to 14–24-h embryos in controls versus *sisR-1* RNAi versus *sisR-1* RNAi + *ASTR* RNAi embryos. Error bars represent SD. *n* = 3. P-value represents *t* test. (E) Model for the regulatory relationship between *sisR-1*, *ASTR*, and *rga* pre-mRNA during embryogenesis.

Materials and methods

Fly strains

The *y w* strain was used as controls unless otherwise stated. Fly strains used were $rga^{EY10731}$ (a P-element insertion in the *rga* locus that allows Gal4-inducible expression; Bloomington 20207), *MTD-Gal4* (a driver that expresses in the germline; Petrella et al., 2007), *da-Gal4* (a driver that expresses ubiquitously), *actin-Gal4* (a driver that expresses ubiquitously), and *UAS-ldbr RNAi* (an RNAi line that knocks down the expression of *ldbr*; Conklin et al., 2005). For embryo collection, females were fed with wet yeast for 1–2 d before mating. They were then mated to males in bottles at 25°C. For generation of dsRed-intron-myc transgenic flies, PCR of full-length intronic sequences was performed using primers that contain the AscI–NotI restriction sites. The PCR product was purified and cut using AscI and NotI, and ligated into AscI–NotI digested UAS-dsRed-intron-myc plasmid (Okamura et al., 2007). Transgenic flies were generated by Genetics Services using P-element–mediated insertion (Rubin and Spradling, 1982). For generation of *sisR-1* and *ASTR* shRNA transgenic flies, design of shRNAs targeting *sisR-1* and *ASTR* and cloning into Valium22 plasmid were performed as previously described (Ni et al., 2011). Sequences were chosen to avoid off-target effects. Transgenic flies were generated by Genetics Services using phiC31 integrase-mediated insertion into 25C7 landing site (Bischof et al., 2007). Oligo sequences are available in Table S2.

RNA extraction

Tissues were homogenized with a plastic pestle in 1.5 ml plastic Eppendorf tubes, and RNA was extracted using the TRIzol extraction protocol (Ambion; Thermo Fisher Scientific), Direct-zol RNA miniprep kit (Zymo Research), or RNeasy plus mini kit (QIAGEN). For deep sequencing, rRNA depletion was performed using the Ribo-Zero magnetic kit (Epicentre). RNA was quantified with the NanoDrop 2000 spectrophotometer (Thermo Fisher Scientific) and further characterized with a Bioanalyzer 2100 (Agilent Technologies).

Sequencing and sequence analysis

Construction of cDNA libraries, sequencing, and analysis were performed as previously described (Gardner et al., 2012). RNA was fragmented, and cDNA library was constructed using random hexamers as primers following the procedure in the Illumina TruSeq RNA sample preparation guide. 100-bp sequencing was performed using the Illumina HiSeq 2000 sequencer. Reads were aligned to the *D. melanogaster* genome (*dm3* genome release) using TopHat version 1.4.0 and Bowtie version 0.12.9 sequence alignment programs (Langmead et al., 2009; Trapnell et al., 2009).

Identification of candidate sisRNAs

Sequenced and aligned reads were passed through a Perl-filtering algorithm to determine if they were internal to an intron or overlapped with the 5′ or 3′ junction of each intron in the *D. melanogaster* (*dm3*) genome. Each intron was indexed, and reads that aligned to the index were parsed and counted to determine molecule size. Sequence information was then extracted for each putative molecule and pairwise aligned using Blast (Altschul et al., 1997). Positive Blast hits were then aligned with Clustalw2 to determine actual sequence alignment for further downstream analysis (Larkin et al., 2007). Candidates with ≤100 reads were first selected because they are less likely to be abundant alternatively spliced mRNAs, snoRNAs, or other annotated ncRNAs.

Candidates were manually checked on the Integrative Genomics Viewer browser (Nicol et al., 2009) with cross-reference to FlyBase to eliminate candidates that might be alternatively spliced mRNAs, intronic or overlapping protein-coding genes, or ncRNAs (including mirtrons, snoRNAs, and long ncRNAs). Furthermore, on visual examination, the reads should cluster at a particular section of the intron to form a discernible peak and not be scattered along the entire intron.

RT-PCR

For standard RT-PCR, total RNA was reverse transcribed for 1 h using AMV-RT (New England BioLabs) or M-MLV RT (Promega) with random hexamers. The cDNA was then used for PCR. For strand-specific RT-PCR, the one-step RT-PCR kit (QIAGEN) was used. RT was performed with a single primer, followed by PCR with both primers at 40 cycles. PCR products were visualized on 1%–2% agarose gels. For qPCR, SYBR Fast qPCR kit master mix (2×) universal (Kapa Biosystems) with addition of ROX reference dye high was used with the Applied Biosystems 7900HT Fast Real-Time PCR system.

5′ RACE and 3′ RACE

For 5′ RACE, a 5′ adaptor was ligated to RNA using T4 RNA ligase (Roche). RT was performed using *sisR-1*–specific reverse primer. For 3′ RACE, poly(U) tailing was performed to RNA using poly(U) polymerase (New England BioLabs). RT was performed using an adaptor containing poly(A). Nested PCR was performed using *sisR-1*– and adaptor-specific primers. PCR products were run on an agarose gel, purified and cloned into pGEM-T-Easy vector (Promega), and sequenced.

Nuclear-cytoplasmic fractionation

Nuclear-cytoplasmic fraction was performed as described previously (Liu et al., 2011). Embryos were dechorionated in 50% bleach for 2 min and washed extensively before homogenization in cold lysis buffer (100 mM potassium acetate, 0.1% Triton X-100, 50 mM Hepes, pH 7.4, 2 mM magnesium acetate, 10% glycerol, 1 mM DTT, and 1× complete mini EDTA-free protease inhibitor cocktail; Roche). Lysate was spun at 1,300 *g* for 10 min at 4°C. The supernatant was collected as the cytoplasmic fraction. The crude nuclear pellet was homogenized in cold lysis buffer and spun at 1,300 *g* for 10 min at 4°C. The resultant pellet was collected as the nuclear fraction. After nuclear-cytoplasmic fractionation, RNA was extracted and dissolved in equal volumes of water. Equal volumes equivalent of RNA were used for Northern blot and RT-PCR analyses.

RNase R treatment

RNA was incubated with 10X RNase R reaction buffer (Epicentre) at 65°C for 5 min to denature the RNA. Samples were then cooled on ice for 2 min before adding 1 µl RNasin (40 U/µl; Promega) and 1 µl RNase R (20 U/µl; Epicentre) and incubated at 37°C overnight.

Northern blotting

For sisRNA analysis, 10–30 µg of total RNA was separated on an 8% denaturing polyacrylamide gel (8 M urea, 1× TBE buffer). RNA was transferred by electrophoresis onto a nylon membrane (Zeta-Probe GT membrane; Bio-Rad Laboratories). For *ASTR* analysis, 8–10 µg of total RNA was separated on a 0.8% agarose/formaldehyde gel. RNA was transferred by capillary action onto a nylon membrane (Zeta-Probe GT membrane; Bio-Rad Laboratories). RNA was then UV cross-linked to the membranes, prehybridized with salmon sperm DNA, and hybridized overnight (14–16 h) with probes in DIG Easy Hyb Granules (Roche) at 51°C (for *mbt* sisRNA) or 42°C (for all other sisRNAs). DIG-labeled DNA probes were synthesized by PCR with genomic DNA as the template and purified before using. After hybridization, the membranes were rinsed once with 2× SSC, followed by one wash with 2× SSC and 0.1% SDS, and two washes with 0.1× SSC and 0.1% SDS. Detection was performed using the CDP-Star chemiluminescent substrate (Roche) and exposed on x-ray films.

Actinomycin D treatment

Ovaries were incubated with 20 µg/ml actinomycin D in Grace's medium with constant rocking at room temperature.

5-ethynyluridine labeling

Ovaries were incubated with 5-ethynyluridine in Grace's medium (1:50) at room temperature. Samples were fixed in 4% paraformaldehyde in Grace's medium for 10 min, rinsed twice in PBST (0.2% Triton X-100), and blocked for 30 min. Detection using Alexa Fluor 488 was performed in accordance with the manufacturer's protocol (Life Technologies). Ovaries were stained with DAPI (4′,6-diamidino-2-phenylindole), mounted in Vectashield (Vector Laboratories), and examined under a fluorescence microscope (Olympus BX61) using 10× dry NA 0.2 and 40× dry NA 0.75 objectives at room temperature. Images were taken using a digital charge couple device camera (C4742-95; Hamamatsu) and acquired using Slidebook 4.1 software and processed (adjustment of brightness and contrast) using ImageJ and Photoshop software.

Accession number

Expression data were deposited in the NCBI Gene Expression Omnibus under accession no. GSE69212.

Online supplemental material

Fig. S1 shows the identification of sisRNAs by RT-PCR and Northern blotting. Fig. S2 shows the characterization of *sisR-1* and *rga* expression. Fig. S3 shows the verification of *sisR-1* knockdown by shRNAs. Table S1 shows a list of candidate sisRNAs in 0–2 h embryos. Table S2 shows a list of oligonucleotides used in this study. Online supplemental material is available at http://www.jcb.org/cgi/content/full/jcb.201507065/DC1.

Acknowledgments

We thank Joseph Gall in whose laboratory these studies were started. We thank Megan Kutzer, Allison Pinder, Nicholas Ingolia, Eugene Gardner, and Fred Tan for help in deep sequencing and bioinformatics, Allan Spradling and members of the Gall, Spradling, Kai, and Pek laboratories for technical support and discussion, Katsutomo Okamura for sharing fly strains, plasmids, and critical reading of the manuscript, and the Bloomington Stock Center. We acknowledge the core facilities at the Carnegie Institution (Department of Embryology) and Temasek Life Sciences Laboratory for their support over the course of this study.

J.W. Pek is a Howard Hughes Medical Institute Fellow of the Life Sciences Research Foundation. The authors are supported by the Temasek Life Sciences Laboratory.

The authors declare no further competing financial interests.

Submitted: 15 July 2015
Accepted: 18 September 2015

References

Altschul, S.F., T.L. Madden, A.A. Schäffer, J. Zhang, Z. Zhang, W. Miller, and D.J. Lipman. 1997. Gapped BLAST and PSI-BLAST: A new generation of protein database search programs. *Nucleic Acids Res.* 25:3389–3402. http://dx.doi.org/10.1093/nar/25.17.3389

Berezikov, E., W.J. Chung, J. Willis, E. Cuppen, and E.C. Lai. 2007. Mammalian mirtron genes. *Mol. Cell.* 28:328–336. http://dx.doi.org/10.1016/j.molcel.2007.09.028

Bischof, J., R.K. Maeda, M. Hediger, F. Karch, and K. Basler. 2007. An optimized transgenesis system for *Drosophila* using germ-line-specific phiC31 integrases. *Proc. Natl. Acad. Sci. USA.* 104:3312–3317. http://dx.doi.org/10.1073/pnas.0611511104

Brown, J.W., D.F. Marshall, and M. Echeverria. 2008. Intronic noncoding RNAs and splicing. *Trends Plant Sci.* 13:335–342. http://dx.doi.org/10.1016/j.tplants.2008.04.010

Bushati, N., and S.M. Cohen. 2007. microRNA functions. *Annu. Rev. Cell Dev. Biol.* 23:175–205. http://dx.doi.org/10.1146/annurev.cellbio.23.090506.123406

Cech, T.R., and J.A. Steitz. 2014. The noncoding RNA revolution-trashing old rules to forge new ones. *Cell.* 157:77–94. http://dx.doi.org/10.1016/j.cell.2014.03.008

Clement, J.Q., L. Qian, N. Kaplinsky, and M.F. Wilkinson. 1999. The stability and fate of a spliced intron from vertebrate cells. *RNA.* 5:206–220. http://dx.doi.org/10.1017/S1355838299981190

Conklin, J.F., A. Goldman, and A.J. Lopez. 2005. Stabilization and analysis of intron lariats *in vivo*. *Methods.* 37:368–375. http://dx.doi.org/10.1016/j.ymeth.2005.08.002

Frolov, M.V., E.V. Benevolenskaya, and J.A. Birchler. 1998. *Regena* (*Rga*), a *Drosophila* homolog of the global negative transcriptional regulator CDC36 (NOT2) from yeast, modifies gene expression and suppresses position effect variegation. *Genetics.* 148:317–329.

Gardner, E.J., Z.F. Nizami, C.C. Talbot Jr., and J.G. Gall. 2012. Stable intronic sequence RNA (sisRNA), a new class of noncoding RNA from the oocyte nucleus of *Xenopus tropicalis*. *Genes Dev.* 26:2550–2559. http://dx.doi.org/10.1101/gad.202184.112

Guil, S., M. Soler, A. Portela, J. Carrère, E. Fonalleras, A. Gómez, A. Villanueva, and M. Esteller. 2012. Intronic RNAs mediate EZH2 regulation of epigenetic targets. *Nat. Struct. Mol. Biol.* 19:664–670. http://dx.doi.org/10.1038/nsmb.2315

Heo, J.B., and S. Sung. 2011. Vernalization-mediated epigenetic silencing by a long intronic noncoding RNA. *Science*. 331:76–79. http://dx.doi.org/10.1126/science.1197349

Herranz, H., and S.M. Cohen. 2010. MicroRNAs and gene regulatory networks: Managing the impact of noise in biological systems. *Genes Dev.* 24:1339–1344. http://dx.doi.org/10.1101/gad.1937010

Herzog, V.A., A. Lempradl, J. Trupke, H. Okulski, C. Altmutter, F. Ruge, B. Boidol, S. Kubicek, G. Schmauss, K. Aumayr, et al. 2014. A strand-specific switch in noncoding transcription switches the function of a Polycomb/Trithorax response element. *Nat. Genet.* 46:973–981. http://dx.doi.org/10.1038/ng.3058

Hoskins, A.A., and M.J. Moore. 2012. The spliceosome: A flexible, reversible macromolecular machine. *Trends Biochem. Sci.* 37:179–188. http://dx.doi.org/10.1016/j.tibs.2012.02.009

Jao, C.Y., and A. Salic. 2008. Exploring RNA transcription and turnover in vivo by using click chemistry. *Proc. Natl. Acad. Sci. USA.* 105:15779–15784. http://dx.doi.org/10.1073/pnas.0808480105

Kim, Y.K., and V.N. Kim. 2007. Processing of intronic microRNAs. *EMBO J.* 26:775–783. http://dx.doi.org/10.1038/sj.emboj.7601512

Kung, J.T., D. Colognori, and J.T. Lee. 2013. Long noncoding RNAs: Past, present, and future. *Genetics.* 193:651–669. http://dx.doi.org/10.1534/genetics.112.146704

Langmead, B., C. Trapnell, M. Pop, and S.L. Salzberg. 2009. Ultrafast and memory-efficient alignment of short DNA sequences to the human genome. *Genome Biol.* 10:R25. http://dx.doi.org/10.1186/gb-2009-10-3-r25

Larkin, M.A., G. Blackshields, N.P. Brown, R. Chenna, P.A. McGettigan, H. McWilliam, F. Valentin, I.M. Wallace, A. Wilm, R. Lopez, et al. 2007. Clustal W and Clustal X version 2.0. *Bioinformatics.* 23:2947–2948. http://dx.doi.org/10.1093/bioinformatics/btm404

Lasko, P. 2012. mRNA localization and translational control in *Drosophila* oogenesis. *Cold Spring Harb. Perspect. Biol.* 4:a012294. http://dx.doi.org/10.1101/cshperspect.a012294

Lee, J.T. 2012. Epigenetic regulation by long noncoding RNAs. *Science.* 338:1435–1439. http://dx.doi.org/10.1126/science.1231776

Leverette, R.D., M.T. Andrews, and E.S. Maxwell. 1992. Mouse U14 snRNA is a processed intron of the cognate hsc70 heat shock pre-messenger RNA. *Cell.* 71:1215–1221. http://dx.doi.org/10.1016/S0092-8674(05)80069-8

Liu, J., and E.S. Maxwell. 1990. Mouse U14 snRNA is encoded in an intron of the mouse cognate *hsc70* heat shock gene. *Nucleic Acids Res.* 18:6565–6571. http://dx.doi.org/10.1093/nar/18.22.6565

Liu, L., H. Qi, J. Wang, and H. Lin. 2011. PAPI, a novel TUDOR-domain protein, complexes with AGO3, ME31B and TRAL in the nuage to silence transposition. *Development.* 138:1863–1873. http://dx.doi.org/10.1242/dev.059287

Matera, A.G., R.M. Terns, and M.P. Terns. 2007. Non-coding RNAs: Lessons from the small nuclear and small nucleolar RNAs. *Nat. Rev. Mol. Cell Biol.* 8:209–220. http://dx.doi.org/10.1038/nrm2124

Moss, W.N., and J.A. Steitz. 2013. Genome-wide analyses of Epstein-Barr virus reveal conserved RNA structures and a novel stable intronic sequence RNA. *BMC Genomics.* 14:543. http://dx.doi.org/10.1186/1471-2164-14-543

Ni, J.Q., R. Zhou, B. Czech, L.P. Liu, L. Holderbaum, D. Yang-Zhou, H.S. Shim, R. Tao, D. Handler, P. Karpowicz, et al. 2011. A genome-scale shRNA resource for transgenic RNAi in *Drosophila*. *Nat. Methods.* 8:405–407. http://dx.doi.org/10.1038/nmeth.1592

Nicol, J.W., G.A. Helt, S.G. Blanchard Jr., A. Raja, and A.E. Loraine. 2009. The Integrated Genome Browser: Free software for distribution and exploration of genome-scale datasets. *Bioinformatics.* 25:2730–2731. http://dx.doi.org/10.1093/bioinformatics/btp472

Okamura, K., J.W. Hagen, H. Duan, D.M. Tyler, and E.C. Lai. 2007. The mirtron pathway generates microRNA-class regulatory RNAs in *Drosophila*. *Cell.* 130:89–100. http://dx.doi.org/10.1016/j.cell.2007.06.028

Peláez, N., and R.W. Carthew. 2012. Biological robustness and the role of microRNAs: A network perspective. *Curr. Top. Dev. Biol.* 99:237–255. http://dx.doi.org/10.1016/B978-0-12-387038-4.00009-4

Petrella, L.N., T. Smith-Leiker, and L. Cooley. 2007. The Ovhts polyprotein is cleaved to produce fusome and ring canal proteins required for *Drosophila* oogenesis. *Development.* 134:703–712. http://dx.doi.org/10.1242/dev.02766

Raabe, C.A., T.H. Tang, J. Brosius, and T.S. Rozhdestvensky. 2014. Biases in small RNA deep sequencing data. *Nucleic Acids Res.* 42:1414–1426. http://dx.doi.org/10.1093/nar/gkt1021

Rinn, J.L., and H.Y. Chang. 2012. Genome regulation by long noncoding RNAs. *Annu. Rev. Biochem.* 81:145–166. http://dx.doi.org/10.1146/annurev-biochem-051410-092902

Rubin, G.M., and A.C. Spradling. 1982. Genetic transformation of *Drosophila* with transposable element vectors. *Science.* 218:348–353. http://dx.doi.org/10.1126/science.6289436

Ruby, J.G., C.H. Jan, and D.P. Bartel. 2007. Intronic microRNA precursors that bypass Drosha processing. *Nature.* 448:83–86. http://dx.doi.org/10.1038/nature05983

Sarot, E., G. Payen-Groschêne, A. Bucheton, and A. Pélisson. 2004. Evidence for a *piwi*-dependent RNA silencing of the *gypsy* endogenous retrovirus by the *Drosophila melanogaster flamenco* gene. *Genetics.* 166:1313–1321. http://dx.doi.org/10.1534/genetics.166.3.1313

Sharp, P.A., M.M. Konarksa, P.J. Grabowski, A.I. Lamond, R. Marciniak, and S.R. Seiler. 1987. Splicing of messenger RNA precursors. *Cold Spring Harb. Symp. Quant. Biol.* 52:277–285. http://dx.doi.org/10.1101/SQB.1987.052.01.033

Spradling, A.C. 1993. Developmental Genetics of Oogenesis. *In* The Development of *Drosophila melanogaster*. A.M. Bate, editor. Cold Spring Harbor Laboratory Press, Cold Spring Harbor, NY. 1–70.

Trapnell, C., L. Pachter, and S.L. Salzberg. 2009. TopHat: Discovering splice junctions with RNA-Seq. *Bioinformatics.* 25:1105–1111. http://dx.doi.org/10.1093/bioinformatics/btp120

Tycowski, K.T., M.D. Shu, and J.A. Steitz. 1993. A small nucleolar RNA is processed from an intron of the human gene encoding ribosomal protein S3. *Genes Dev.* 7:1176–1190. http://dx.doi.org/10.1101/gad.7.7a.1176

Wahl, M.C., C.L. Will, and R. Lührmann. 2009. The spliceosome: Design principles of a dynamic RNP machine. *Cell.* 136:701–718. http://dx.doi.org/10.1016/j.cell.2009.02.009

Wight, M., and A. Werner. 2013. The functions of natural antisense transcripts. *Essays Biochem.* 54:91–101. http://dx.doi.org/10.1042/bse0540091

Xue, Z., Q. Ye, S.R. Anson, J. Yang, G. Xiao, D. Kowbel, N.L. Glass, S.K. Crosthwaite, and Y. Liu. 2014. Transcriptional interference by antisense RNA is required for circadian clock function. *Nature.* 514:650–653. http://dx.doi.org/10.1038/nature13671

Yin, Q.F., L. Yang, Y. Zhang, J.F. Xiang, Y.W. Wu, G.G. Carmichael, and L.L. Chen. 2012. Long noncoding RNAs with snoRNA ends. *Mol. Cell.* 48:219–230. http://dx.doi.org/10.1016/j.molcel.2012.07.033

Zhang, Y., X.O. Zhang, T. Chen, J.F. Xiang, Q.F. Yin, Y.H. Xing, S. Zhu, L. Yang, and L.L. Chen. 2013. Circular intronic long noncoding RNAs. *Mol. Cell.* 51:792–806. http://dx.doi.org/10.1016/j.molcel.2013.08.017